

Measurement and theoretical analysis of solar temperature field in steel-concrete composite girder

Chen Xiaoqiang¹ Liu Qiwei¹ Zhu Jun²

(¹School of Transportation, Southeast University, Nanjing 210096, China)

(²Anhui Communications Consulting & Design Institute, Hefei 230031, China)

Abstract: The solar temperature field of a large three-span continuous bridge with steel-concrete composite box girder and variable cross-section is measured to verify a calculation method for the temperature field of steel-concrete composite beams. The test results show that the temperature of an external steel web-plate is higher than that of an internal web-plate due to the difference in solar radiation. Air temperature inside the box matches the average temperature of the whole steel box. Based on actual measurements, a transient thermal analysis with multiple boundary conditions is also carried out by a software program ANSYS. Convective boundary situation and states of solar radiation on steel web plates in different situations are determined in the analysis. The feature of the temperature field is preliminarily achieved through a comparative study between the actual measurement and the finite element analysis. The computed results are in good consistence with the actual measurement results, with the maximum difference within 2 °C. This indicates that the theoretical calculation method is reliable and it provides a foundation for further research on temperature field distribution in the steel-concrete composite box girder.

Key words: steel-concrete composite structure; solar radiation; temperature field; experiment

Many researches on the temperature field of the concrete box girder have been conducted in past decades, which have resulted in many achievements. In 1998, based on a five-year testing study, Shushkewich^[1] proposed a simplified method for calculating the temperature gradient and stress in a section of a prestressed concrete viaduct, which provided a reference for a revision of corresponding AASHTO specifications. Little work, however, has been carried out on the solar temperature field in steel-concrete composite box beams. In some bridge design specifications^[2], the vertical temperature gradient in steel-concrete composite box girder bridges uses the same mode as for that in concrete bridges. The actual heat transfer characteristics of steel, however, are different from those of concrete. It is, therefore, necessary to conduct further research to investigate the differences.

With the support from a real project, this paper focuses on the field test and the theoretical calculation of the temperature field in steel-concrete composite box girders. Considering different boundary conditions (such as solar radiation, internal and external air temperature, and convective heat transfer of

air) and physical material parameters, theoretical calculation is carried out using a software program ANSYS. The analysis results match field measurements well, which provides a foundation for further research of temperature field distribution in steel-concrete composite box girders.

1 General Situation of Bridge

Located on Dantu, Zhenjiang, the steel-concrete composite box girder bridge has three different spans with two separated superstructures and variable cross-sections. The width of the superstructure deck is 13.5 m, and the thickness of the concrete deck-slab is 0.41 m. The height of the girder is variable in the form of a parabolic curve, which is 1.5 m at mid-span and 2.7 m at pier. The steel web-plates of each separated superstructure are affected by eastern or western sunshine because the bridge runs in a north-south direction. One section near the east-side pier is selected for temperature measurement (see Fig. 1 and Fig. 2). According to the engineering schedule, the temperature data on Sept 17, 2004 was measured and recorded.

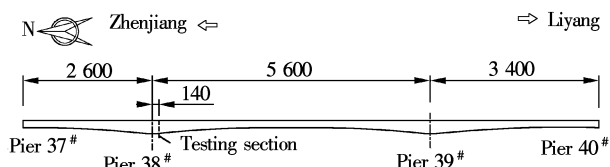


Fig. 1 Elevation view of east-deck bridge (unit: cm)

2 Boundary Conditions and Concerned Parameters

The main factors that influence the structural temperature-field are the intensity of solar radiation, air temperature, and wind speed in certain situations including geographical latitude, position angle, time and terrain condition. The intensity of solar radiation is the main factor that affects the increase in the structural temperature, and it can be obtained from a weather observations. Wind reduces the structural surface temperature. Wind speed, which concerns the heat exchange coefficient of the surface in calculation, can also be obtained from the observations. Generally, it is not necessary to obtain highly accurate measurements of wind speed. Air temperatures inside and outside the box can be easily measured with temperature sensors in place.

2.1 Intensity of solar radiation

Offered by Jiangsu Provincial Meteorology Bureau, states of solar radiation are shown in Tab. 1. The elevation angle of the sun at different time is calculated according to the longitude (119.45°) and latitude (32.04°) of the bridge location^[3-4]. The table shows that the intensity of solar radiation

Received 2009-02-13.

Biography: Chen Xiaoqiang (1973—), male, graduate, lecturer, cxq_se@yahoo.com.cn.

Citation: Chen Xiaoqiang, Liu Qiwei, Zhu Jun. Measurement and theoretical analysis of solar temperature field in steel-concrete composite girder [J]. Journal of Southeast University (English Edition), 2009, 25(4): 513–517.

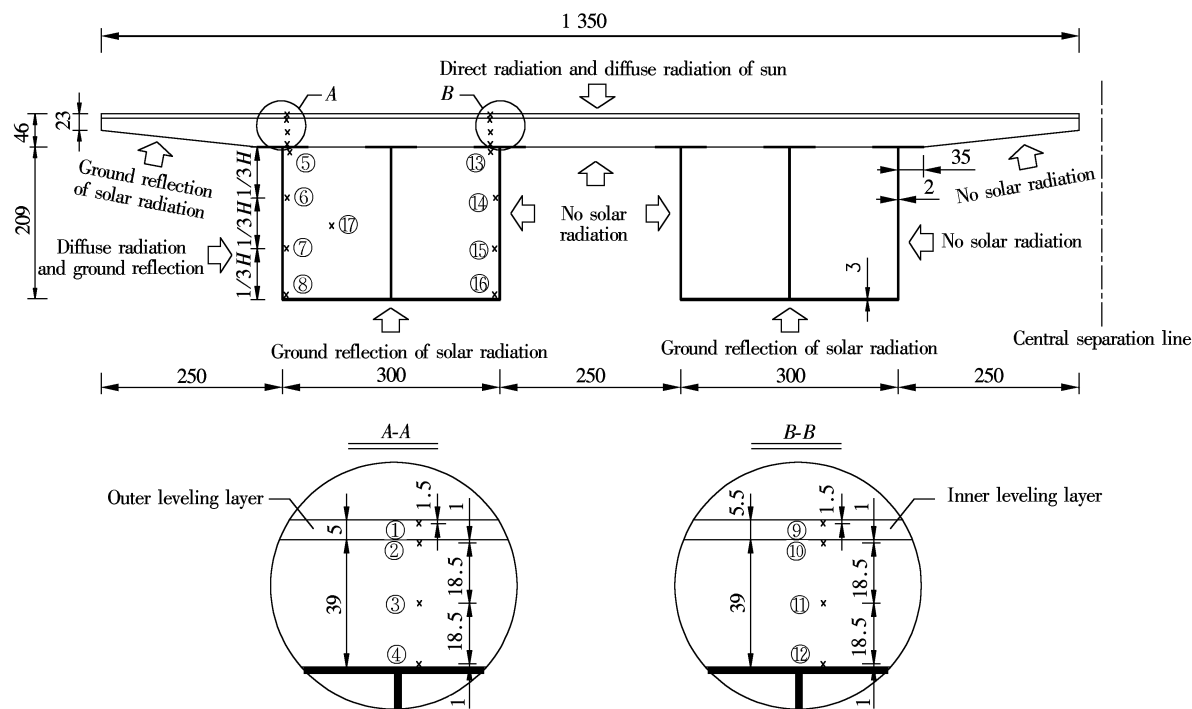


Fig. 2 Layout of temperature sensors and states of solar radiation(unit: cm)

varied slightly in the morning before ten o'clock. This was due to the existence of some fog. After ten o'clock, the radiation intensity increased due to the gradual disappearance of the fog. Fig. 3 shows the actual intensity curve of solar radiation and a restored curve based on symmetry.

Tab. 1 States of solar radiation on Sept 17, 2004

Beijing time	Hour angle/(°)	Elevation angle of sun/(°)	Intensity of solar radiation/(W·m ⁻²)	Horizontal intensity of solar radiation/(W·m ⁻²)
6:00	-90	0.98	2.78	0.05
8:00	-60	26.16	58.33	25.72
10:00	-30	48.69	263.89	198.22
11:00	-15	56.70	591.67	494.52
12:00	0	59.84	733.33	634.06
13:00	15	56.70	769.44	643.11
14:00	30	48.69	702.78	527.89
16:00	60	26.16	391.67	172.68
18:00	90	0.98	33.33	0.57

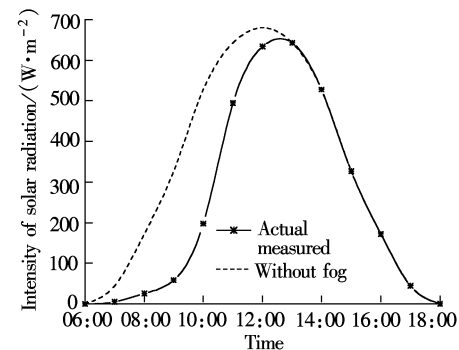


Fig. 3 Horizontal intensity of solar radiation

Domestic and foreign researchers have determined different values for the solar radiation absorption coefficient of a

concrete surface. For example, 0.65 appeared in Ref. [5], and 0.5 was suggested by experiments in Ref. [6]. In this paper, 0.55 is adopted for the purpose of calculation. The solar radiation absorption coefficient of the steel surface with coating is chosen as 0.4. The solar radiation is applied by time sequence as the heat flux density for the computation model.

2.2 Internal and external air temperatures

The temperature on Sept 17, 2004 varied between 22 and 32 °C. The detailed data, as shown in Tab. 2 and Fig. 4, are also provided by the meteorology bureau. It is obvious in Fig. 3 and Fig. 4 that the variation of air temperature coincides with the variation of solar radiation. The actual temperature curve differs from the standard curve because of the effect of fog. Air temperature inside the box is measured via temperature sensors (see Fig. 2).

At night, the air temperatures above and below the bridge were almost identical. During the day, the air temperature below the bridge was lower than that of sheltered air temperature. For convenience, the maximal temperature difference between the air below the bridge and the ordinary sheltered air was assumed to be 3 °C, and the air tempera-

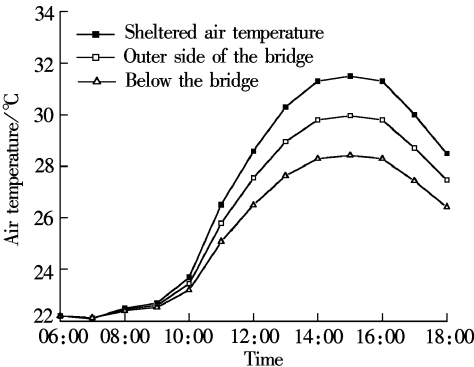


Fig. 4 Variation of air temperature

ture near the extra-web-plate took the average value of the sheltered air temperature and the air temperature below bridge, as shown in Fig. 4.

Tab. 2 Air temperatures for temperature field calculation °C

Beijing time	Sheltered air temperature	Outer side of the bridge	Below bridge	Inside the box
6: 00	22. 2	22. 2	22. 2	24. 1
8: 00	22. 5	22. 5	22. 4	24. 5
10: 00	23. 7	23. 5	23. 2	25. 0
12: 00	28. 6	27. 5	26. 5	25. 9
14: 00	31. 3	29. 8	28. 3	27. 9
16: 00	31. 3	29. 8	28. 3	28. 0
18: 00	28. 5	27. 5	26. 4	27. 9

2.3 Heat convection of air

The coefficient of heat transfer between the air and the structural surface can be calculated by^[3]

h≈2. 6(4√ΔT +1. 54v) (1)

where v is the wind speed, and v≤5.0 m/s; ΔT is the difference between the structural surface temperature and the air temperature near the surface.

On Sept 17, 2004, the wind speed was very low, so a value of 1.0 m/s was adopted for calculation. The air temperatures are listed in Tab.2, in which “shelter weather temperature” is adopted for the top surface of the bridge; “below bridge” is adopted for the bottom and internal-side web plate; and “external side below the bridge” is adopted for the outside web-plate. Fig. 5 shows the dynamic variation of the convection coefficient between the air and the structural surface. The coefficient inside the box is 4.74 W/(m²·K)^[7], because the internal air is almost still.

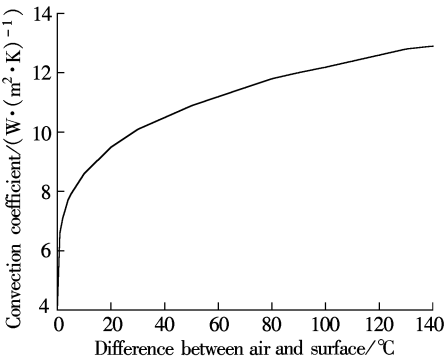


Fig. 5 Curve of convection coefficient

2.4 Heat engineering coefficient

The steel fiber was added, at a rate of 50 kg fiber in 1 m³ concrete, into the concrete to improve the toughness of the concrete and increase the heat conductivity. Because the volumetric content of the steel fiber is 0.64%, and the thermal diffusivity of the steel-fiber concrete is 0.003 9 m²/h^[8], the calculated coefficient of the heat conductivity is 2.2 W/(m²·K). Heat engineering coefficients of other materials are listed in Tab. 3.

2.5 Initial temperature condition

After the sun rises on a sunny day, the structure absorbs solar radiation energy and the temperature rises gradually. When

Tab. 3 Heat engineering coefficients of other materials

Material	Density/(kg·m ⁻³)	Coefficient of heat conductivity/(W·(m ² ·K) ⁻¹)	Specific heat/(J·(kg·K) ⁻¹)
Polypropylene fibre concrete	2 300	1.7	920
Steel-fibre concrete	2 500	2. 2	900
16 Mn steel	7 850	58. 2	480 ^[9]

the temperature of the top surface reaches the maximum at a moment after noon, its absorption of solar radiation energy begins to decrease. After sunset, the structure starts to release heat to the external environment, which leads to a quick temperature decrease. Since then, the internal temperature remains higher than the external temperature until the next sunrise. On Sept 17, 2004, the internal temperature was still higher than the external temperature before 07:00, so the temperature measured at 6:00 was determined as the initial condition.

3 Measurement and Comparative Analysis

For a straight bridge, the boundary conditions of each cross-section are similar, and the measured longitudinal temperatures are almost the same. Therefore, the transverse flat model is adaptable for calculating the solar temperature field. In order to verify the method, a comparative analysis between the field measurement and the theoretical modeling is carried out for heat engineering coefficients of materials and the accuracy of boundary conditions.

3.1 Feature of temperature

The following features can be observed from Fig. 6 and Fig. 7:

- 1) The temperature of the top surface increases gradually

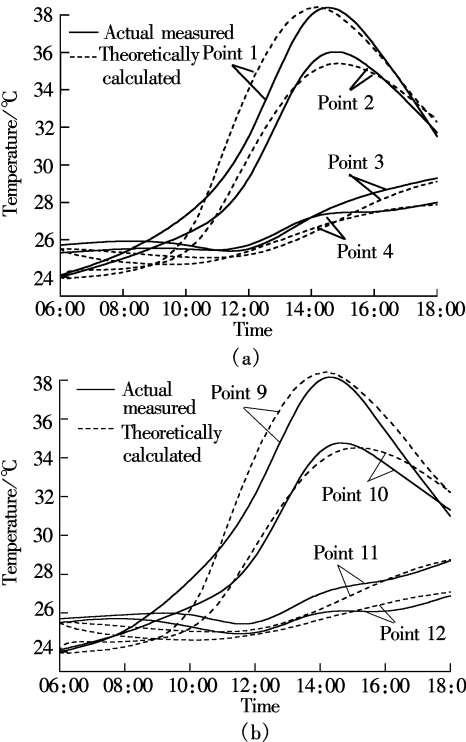


Fig. 6 Temperature in deck slab of tests and calculations. (a) Internal points; (b) External points

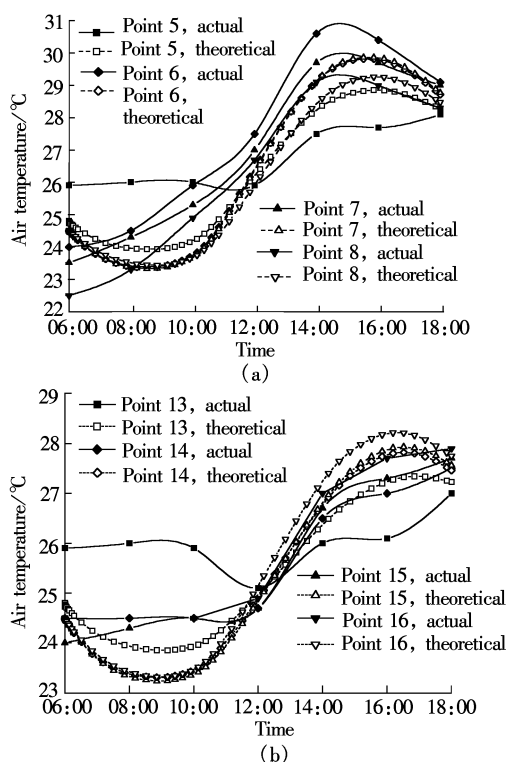


Fig. 7 Temperature in steel web-plate of tests and calculation. (a) Internal points; (b) External points

with the increase in solar radiation intensity. Also, the temperature of the steel girder rises slowly with air temperature. The temperature of the top surface of the concrete deck-slab reaches the maximum value at about 14:30.

2) The closer a point is to the upper surface, the more fluctuating its temperature is. The temperature fluctuation range is 14 °C for the top deck and 3.5 °C for the middle deck in a day.

3) The temperature of the web-plate on the same side is uniform. The temperature difference is within 1 °C among the testing points of the internal steel web-plate on the same side, and within 2 °C for the external steel web-plate.

4) The direct radiation, diffuse radiation and ground reflection of sun in the internal web-plate are less than those in the external web-plate, because the internal web-plate is sheltered more. Due to the existence of fog in the morning, the temperature difference between the external and internal web-plates is not evident. But after the fog clears, the external temperature is higher than the internal temperature (see Fig. 7). This difference in the radiation of each web-plate must be considered in theoretical calculations.

5) The air temperature inside the box matches the average temperature of the whole steel box (see Fig. 8).

3.2 Theoretical calculation

Based on the calculation parameters and boundary conditions discussed in the previous sections, transient thermal analysis is conducted with ANSYS^[10]. A model is established according to the actual section (see Fig. 2). A Plane55, 2-D thermal solid element is used for modeling the concrete deck-slab and the steel box-girder. A Surf151, 2-D thermal surface effect element is used for modeling various loads and surface effect applications on the same sur-

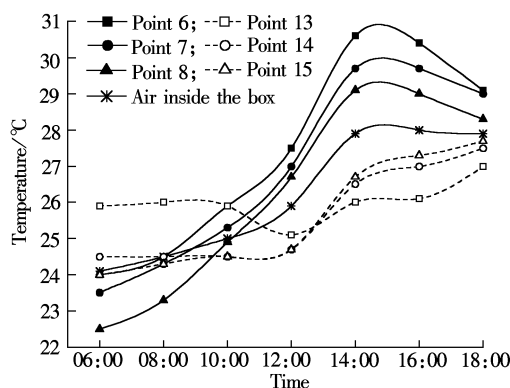


Fig. 8 Temperature curves of steel web-plate and air inside the box

face, including heat flux density, convection and radiation. A Surf151 element is overlaid onto a face of the Plane55 element.

As a heat flux load, solar radiation is applied on the faces of the Plane55 element. The Surf151 element allows convection and radiation between the surface and the air. The heat flux density, convective film coefficient, and extra-air temperature are input in a form of a time-dependent array. The solar radiation on each structural surface is different, as shown in Fig. 2.

3.3 Comparison with measurements

In general, the calculation results coincide with the measurements, as shown in Fig. 6 and Fig. 7. The maximum difference is within 2 °C, excluding single points on the upper steel web-plate.

The actual measurement curves of the No. 5 and the No. 13 points are gentle, but the calculated curves fluctuate more significantly. This is because there is some difference in convection conditions. The actual temperature of the upper air is slightly higher than those of the center and lower air in the box, and the degree of convection is less. For convenience, the same air temperature and convection coefficient are adopted in the calculations. The difference is not obvious and the location is so close to the centroid axis of the whole cross-section that it can be ignored in mechanical analysis.

Before 12:00, the calculated temperature of the steel web is smaller than the actual value. This is because the direct solar radiation is not input in the calculating model, and the external web is directly radiated by sun. But after 12:00, the average temperature of the calculated temperature coincides with the actual value.

In summary, the calculation method, with boundary conditions and choice of heat engineering coefficients discussed in this paper, is reliable for temperature computing. Further research may be conducted based on this method.

4 Conclusions

The features of solar radiation, radiation and convection heat transfer between the bridge surface and the air, the internal and external air temperature variation and the initial temperature field of a structure are discussed in this paper. The regular pattern of the temperature in a steel-concrete composite section is revealed. Through field experimental

study and theoretical calculation, the following conclusions can be drawn:

- 1) Air temperature inside the box matches the average temperature of the whole steel box, which is helpful to determine the internal air temperature mode for calculation.
- 2) The difference in the radiation of each web-plate among different conditions of direct radiation, diffuse radiation and ground reflection must be considered in boundary conditions for theoretical calculation.
- 3) The calculation method with boundary conditions and choice of heat engineering coefficients mentioned in this paper is reliable for temperature computation.

References

[1] Shushkewich K W. Design of segmental bridge for thermal gradient[J]. *PCI Journals*, 1998, **43**(4): 120 – 137.

[2] Ministry of Transport of the People’s Republic of China. General code for design of highway bridges and culverts [S]. Beijing: China Communications Press, 2004. (in Chinese)

[3] Kehlbeck F, Liu Xinfu. *The effect of solar radiation on bridge* [M]. Beijing: China Railway Publishing House, 1981. (in Chinese)

[4] State Environmental Protection Administration of China. Technical guidelines for fugitive emission monitoring of air pollutants[S]. Beijing: China Environmental Science Press, 2001. (in Chinese)

[5] Fu H C, Ng S F, Cheung M S. Thermal behavior of composite bridges [J]. *Journal of Structural Engineering*, 1990, **116**(12): 3302 – 3323.

[6] Zhang Jianrong, Xu Xiangdong, Liu Wenyan. A test study on the solar radiation absorption coefficient of concrete surface[J]. *Building Science*, 2006, **22**(1): 42 – 45. (in Chinese)

[7] Zhang Jianrong, Liu Zhaoqiu, Liu Wenyan. Experimental research on natural convective coefficient of concrete surface [J]. *Sichuan Building Science*, 2007, **33**(5): 143 – 146. (in Chinese)

[8] Mei Mingrong, Yang Yong, Wang Shanshan, et al. Study of thermal property of steel-fiber concrete and its crack-resistance capacity [J]. *Journal of Hydraulic Engineering*, 2007(S1): 111 – 117. (in Chinese)

[9] Ministry of Construction of the People’s Republic of China. Thermal design code for civil building[S]. Beijing: China Planning Press, 1993. (in Chinese)

[10] Zhang Caohui. *Tutorials and examples of thermal analysis by ANSYS 8.0* [M]. Beijing: China Railway Publishing House, 2005. (in Chinese)

钢-混凝土组合箱梁日照温差的实测和理论分析

陈晓强¹ 刘其伟¹ 朱 俊²

(¹ 东南大学交通学院, 南京 210096)

(² 安徽省交通规划设计研究院, 合肥 230031)

摘要: 为了探讨和验证钢-混凝土组合截面日照温度场的计算方法, 依托某大跨径三跨变截面连续箱梁桥, 对钢-混凝土组合箱梁的日照温度场进行了现场实测. 通过实测发现, 由于各腹板接受太阳漫散射的程度不同, 外侧钢梁温度普遍高于内侧箱梁, 且钢箱的整体平均温度数值与箱内空气基本吻合. 在此基础上借助 ANSYS 有限元计算软件, 根据不同位置钢腹板所处环境条件确定了各自的太阳辐射和对流换热情况, 进行了综合边界条件的瞬态热分析. 各测点理论计算结果与实测数据能较好地吻合, 温度差值在 2℃ 以内, 说明了理论计算方法的可靠性, 为后续深入研究钢-混凝土组合截面日照温度场奠定了基础.

关键词: 钢-混凝土组合结构; 太阳辐射; 温度场; 试验

中图分类号: U448.38